The Vertex Tracker at the e^+e^- Linear Collider

Conceptual Design, Detector R&D and Physics Performances for the Next Generation of Silicon Vertex Detectors

Marco Battaglia

Department of Physics, High Energy Physics Division
University of Helsinki, Finland
E-mail: Marco.Battaglia@cern.ch

Massimo Caccia

Dipartimento di Fisica
Universita' dell'Insubria, Como, Italy
E-mail: Massimo.Caccia@mi.infn.it

Abstract

The e^+e^- linear collider physics programme sets highly demanding requirements on the accurate determination of charged particle trajectories close to their production point. A new generation of Vertex Trackers, based on different technologies of high resolution silicon sensors, is being developed to provide the needed performances. These developments are based on the experience with the LEP/SLC vertex detectors and on the results of the R&D programs for the LHC trackers and also define a further program of R&D specific to the linear collider applications. In this paper the present status of the conceptual tracker design, silicon detector R&D and physics studies is discussed.

---

1 Introduction

With the end of the SLC and LEP operations and the commissioning of the B-factories, the next frontier in e^+e^- collisions is set by a high luminosity, high energy linear collider capable of delivering beams at centre-of-mass energies in the range 0.3 TeV $< \sqrt{s} <$ 1.0 TeV with luminosities in excess to 10^{34} cm^{-2} s^{-1}. Expected to be commissioned by the end of the first decade of the new millennium, the linear collider will complement the physics reach of the Tevatron and LHC hadron colliders in the study of the mechanism of electro-weak symmetry breaking and in the search for new physics beyond the Standard Model [1]. Both precision measurements and particle searches set stringent requirements on the efficiency and purity of the flavour identification of hadronic jets since final states

including short-lived b and c-quarks and τ leptons are expected to be the main signatures. High accuracy in the reconstruction of the charged particle trajectories close to their production point must be provided by the tracking detectors, in particular by the Vertex Tracker located closest to the interaction point, in order to perform the reconstruction of the topology of secondary vertices in the decay chain of short-lived heavy flavour particles [2].

If a Higgs boson exists with mass below 150 GeV/c^2, as indicated by the fit to the present electro-weak data [3], it will be essential to carry out precision measurements of its couplings to different fermion species as a proof of the mass generation mechanism and to identify its Standard Model or Supersymmetric nature [4]. This can be achieved by accurate determinations of its decay rate to $b\bar{b}$, $c\bar{c}$, $\tau^+\tau^-$, W^+W^- and gluon pairs to detect possible deviations from the Standard Model predictions [5, 6]. Since the rates for the Higgs decay modes into lighter fermions $h^0 \to c\bar{c}$, $\tau^+\tau^-$ or into gluon pairs are expected to be only about 10% or less of that for the dominant $h^0 \to b\bar{b}$ process, the extraction and measurement of the signals of these decay modes requires suppression of the $b\bar{b}$ contribution by a factor of twenty or better while preserving a good efficiency.

The measurement of the top Yukawa coupling as well as the top-quark mass measurement will require efficient b-tagging to reduce combinatorial background in the reconstruction of the six and eight jet final states. If Supersymmetry is realized in nature, the study of its rich Higgs sector will also require efficient identification of b-jets and τ leptons to isolate the signals for the decays of the heavier A^0, H^0 and $H^\pm$ bosons from the severe combinatorial backgrounds in the resulting complex multi-jet hadronic final states. Due to the large expected b-jet multiplicity, highly efficient tagging is required to preserve a sizeable statistics of the signal events. Finally, both b and c-tagging will be important in the study of the quark scalar partners, while τ identification may be instrumental in isolating signals from Gauge Mediated Supersymmetry Breaking.

Due to the large boost in typical 4-jet events at $\sqrt{s} = 0.5$ TeV, short-lived B, D and τ particles have large decay distances. These are significantly larger compared to those at LEP/SLC, the average boost of B hadrons increasing from $\simeq 6$ to $\simeq 20$. An useful figure of merit of the ability to identify secondary particles is the resolution on the impact parameter σ_{IP}, defined as the distance of closest approach of the extrapolated particle trajectory to the e^+e^- annihilation point. This resolution can be parametrised as the convolution of an asymptotic term $\sigma_{asymptotic}$, depending on the sensor single point resolution and the detector geometry, with a multiple scattering term σ_{ms}, depending on the thickness of the sensor and of its support structure: $\sigma_{I.P.}^{R-\phi(R-z)} = \sigma_{asymptotic} \oplus \frac{\sigma_{m.s.}}{p\ \sin^{3/2(5/2)}\theta}$ where p is the particle momentum and θ its polar angle. In Table 1 the average charged decay multiplicity, decay distance in space, and track impact parameter are summarised. Heavy particle identification relies on the accurate extrapolation of the particle trajecto-

Table 1: The average decay charged multiplicity, decay distance in space and track impact parameter for B, D and τ decays in four jet events at $\sqrt{s} = 500$ GeV

Decay	$< N_{sec} >$	$< d_{space} >$ (cm)	$< IP_{R-\phi} >$ (μm)
$B \to X$	4.9	0.8	450
$D \to X$	2.3	0.4	150
$\tau^\pm \to X$	1.3	0.1	40

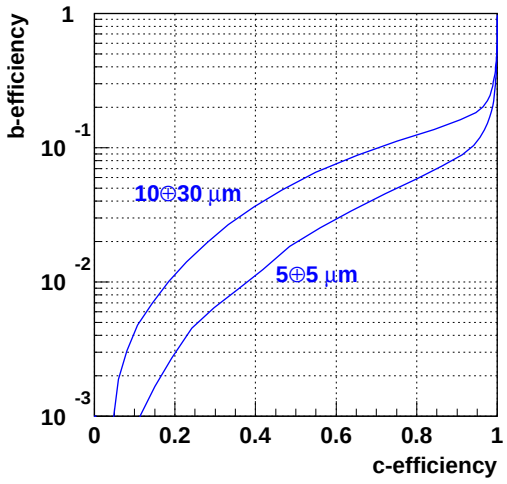

Figure 1: The b-quark background efficiency as a function of the c-quark signal efficiency for a c-tag algorithm based on topological vertexing and impact parameters, developed on the basis of the experience from the SLC and LEP experiments. The two curves show the expected performance for two different assumptions on the track impact parameter resolution.

ries to their production point to identify secondary decay particles from those produced at the primary vertex in the hadronisation process. Efficient tagging of short-lived τ leptons requires very accurate impact parameter resolution for a single high momentum particle in order to discriminate single-prong τ decays from electrons and muons. From the typical impact parameters given in Table 1, a resolution $\sigma_{asymptotic} < 10$ μm is required. On the contrary the decay multiplicity of B and D particles is large enough to perform inclusive reconstruction of decay vertices and efficient b/c flavour separation relies on the distinctive differences in secondary vertex topology, invariant mass and charged decay multiplicity between beauty and charm hadrons. In order to fully exploit these features, sensitivity to 1 GeV/c $< p <$ 3.5 GeV/c particles originating at secondary or tertiary vertices must be retained. From the typical impact parameter difference for B and D decay products, requiring > 3 σ_{IP} separation for the majority of the particles implies value of $\sigma_{ms} < 30$ μm. As an exemplification of these requirements, the performance of a charm-tagging algorithm is shown in Figure 1 for two assumptions on the impact parameter resolution. Due to the forward enhanced cross-section of several processes of interest, such as $e^+e^- \rightarrow WW \rightarrow H^0\nu\bar{\nu}$, and of the $\gamma\gamma$ background, the Vertex Tracker must provide tagging capabilities for polar angles down to $\cos\theta \simeq 0.95$. Lepton charge determination in $e^+e^- \rightarrow W^+W^- \rightarrow X\ell\bar{\nu}$ decays and luminosity measurement by large angle Bhabha scattering require the extension of tracking coverage down to $\cos\theta \simeq 0.99$.

These motivations have promoted a significant amount of studies on the Vertex Tracker conceptual design, the choice of the detector technology and the definition of the needs of dedicated R&D and the evaluation of its physics performances. Contrary to most of the other detector components, such as the main tracking chamber or the calorimeters for which the linear collider specifications can be addressed with technologies already devel-

oped for the LEP/SLC and LHC experiments, the Vertex Tracker sets very challenging requirements that can only be met by a detector of new generation. Therefore, an active programme of studies is presently carried out by US, Asian and European groups defining the design of the detectors for a future linear collider [7]. In this paper we review the present status of the conceptual design, detector R&D and physics performances of the Vertex Tracker design for the TESLA e^+e^- collider project. The next chapter presents the predicted experimental conditions at the TESLA interaction region. In chapter 3 the proposed solutions for the silicon sensor technology and the tracker conceptual designs are reviewed. The last chapter summarises the estimated performances and their impact on Higgs boson physics.

2 Backgrounds and Physics events at the TESLA e^+e^- collider

The TESLA project [8] is based on the use of superconducting accelerating structures that deliver very long beam pulses ($\sim 900\ \mu$s), each accelerating a train of up to 4500 bunches. This scheme allows a large bunch spacing (190-340 ns) making it possible, for the detector, to resolve single bunch crossings (BX) and to perform fast bunch-to-bunch feedback needed to stabilise the beam trajectory within a train, thus preserving the nominal luminosity of (3 - 5) $\times 10^{34}$ cm^{-2} s^{-1}. The large luminosity of each individual bunch-crossing and the large number of bunches in a single pulse imply a high rate of background events that needs to be minimised by a Vertex Tracker with very high granularity and fast time stamping to identify the bunch corresponding to the physics event of interest. While there are several sources of backgrounds, the most relevant for this discussion are the incoherent pair creation, neutrons and $\gamma\gamma$ backgrounds [9].

Low energy e^+e^- pairs are created in the e.m. interaction of the colliding beams by the $\gamma\gamma \to e^+e^-$ (Breit-Wheeler), $e^\pm\gamma \to e^\pm e^+e^-$ (Bethe-Heitler) and $e^+e^- \to e^+e^-e^+e^-$ (Landau-Lifschitz) processes [10]. The generated electrons and positrons are confined spiralling at small radii by the solenoidal magnetic field of the experiment. The number of particles from pairs, intercepting a surface at a given radius depends on the intrinsic transverse momentum of the pairs and on their deflection from the e.m. interaction with the opposite beam. Particles are thus confined in an envelope defined by the maximum angle of deflection and by the strength of the magnetic field B. For the design of the Vertex Tracker the two main parameters of interests are the maximum radius R_{max} of the envelope and its longitudinal position of crossing z_c with a reference surface located at radius R. These define the minimum radius and maximum length of the innermost detector layer and can be expressed in terms of the simple scaling laws [11]:

$$R_{max}[cm] = 0.35\sqrt{\frac{N}{10^{10}}\frac{1}{B[Tesla]}z[cm]\frac{1}{\sigma_z[mm]}} \tag{1}$$

$$z_c[cm] = 8.3\ R^2 B[Tesla]\sigma_z[mm]\frac{10^{10}}{N}. \tag{2}$$

where N is the number of particles in one bunch, B is the magnetic field strength and σ_z the bunch length. Detailed simulation for the case of the TESLA collider at $\sqrt{s} =$ 500 GeV and with $B = 3$ T, shows that the density of hits generated by pairs at a radius

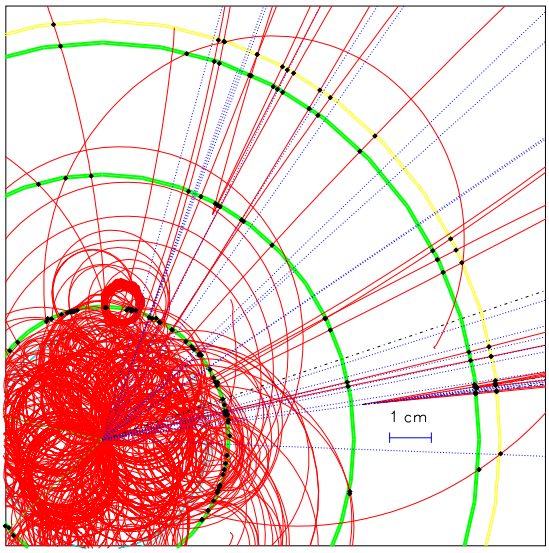

Figure 2: A simulated $e^+e^- \rightarrow Z^0H^0$; $Z^0 \rightarrow \mu^+\mu^-$, $H^0 \rightarrow b\bar{b}$ event at $\sqrt{s} =$ 500 GeV overlayed to the pair backgrounds. The high track density and the distinctive structure of secondary vertices from the B hadron decays are clearly visible. It is interesting to point out that 20% of the B hadrons in such events will decay after having traversed the innermost Vertex Tracker layer.

of 1.2 cm from the interaction point corresponds to $\simeq 0.2$ hit mm^{-2} BX^{-1} and that the longitudinal positions of the pair envelope crossing point on a scoring cylinder at this radius are at ± 7 cm. In addition to the pairs, dense hadronic jets in high multiplicity events, such as $e^+e^- \rightarrow t\bar{t}$; $t \rightarrow Wb$, $W \rightarrow q\bar{q}'$ contribute to the detector occupancy. It has been calculated that at $R = 3.0$ cm about 20% (10%) of the particles in a jet have at least one additional hit within a 150 μm distance in the $R-\phi$ ($R-z$) plane. These results rule out the application of silicon microstrip detectors and highlight the importance of detectors with small sensitive cells, such as pixel sensors.

Another source of background to be taken into account in the choice of the detector technology is the flux of neutrons photo-produced at the dump of electrons from pairs and radiative Bhabha scattering and of beamstrahlung photons. Photons in electro-magnetic showers, lead to the release of fluxes of neutrons through giant dipole resonance excitation, pseudo-deuteron mechanism and photo-pion reaction. Neutrons may induce permanent radiation damage to semiconductor devices by nuclear interactions generating displacement damage of the bulk material. Bulk damage results in charge collection and charge transfer inefficiency (CTI) in the detector structure. CTI affects in particular devices such as the CCDs, where the ionisation charge typically undergoes several thousands transfers before reaching the output node. The computation of the neutron flux at the interaction region relies on the modelling of their production and transport in the accelerator tunnel and in the detector and it is still subject to significant uncertainties. Estimated fluxes are of the order of a few 10^9 n (1 MeV) cm^{-2} year^{-1} [12, 13], where the anticipated neutron flux has been normalised in terms of equivalent 1 MeV neutrons assuming NIEL scaling.

Finally the cross-section for two photon events, at the linear collider energies, is many orders of magnitude larger compared to that of e^+e^- annihilation events. Due to the large luminosity per bunch crossing obtained by TESLA, $L = 2.2 \times 10^{-3}$ nb^{-1} BX^{-1}, the

probability for a $\gamma\gamma \rightarrow jets$ event overlapping with a physics event is 0.09 - 0.14 $\times$ n_{BX}, where n_{BX} is the number of bunch crossings integrated in a detector read-out cycle. Two photon events, depositing a significant energy in the forward regions, can seriously interfere with the identification of physics processes whose signature is missing energy such as $e^+e^- \rightarrow H^0\nu\bar{\nu}$ and SUSY decays and result in an important source of systematics for cross-section measurements. Therefore single bunch identification is highly desirable in order to minimise this background.

3 Detector technologies and Vertex Tracker conceptual designs

The linear collider Vertex Tracker must be able to provide a track impact parameter resolution better than 10 [illegible] and $R - z$ projections for jet flavour identificatio [illegible] μm^2 or less to keep the occupancy from pairs and [illegible]ly identify single bunch crossings separated by abo[illegible]kgrounds. There are two types of such silicon sensor[illegible], that have the potential to satisfy these specificatio[illegible]ve been already proposed for this application: Hybri[illegible] detectors bump-bonded to their VLSI read-out ch[illegible] CCD) [17]. In addition Monolithic CMOS sensors [illegible]4, 16].

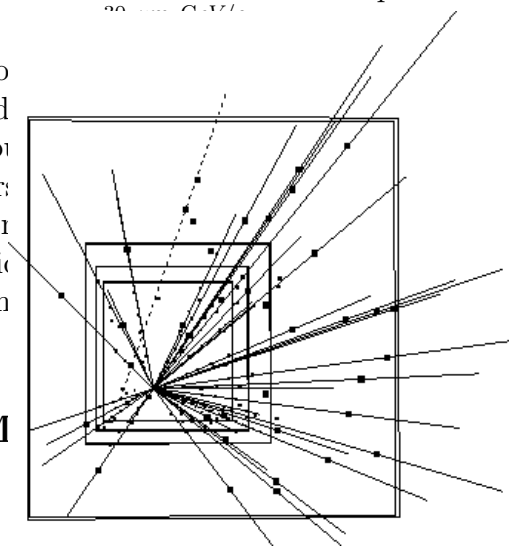

3.1 Hybrid and M[illegible]

Figure 3: Two examples of applications of hybrid pixels sensors: an event of Pb-Pb collision recorded by the WA97 pixel telescope [18] (left) and an hadronic event with tracks reconstructed by the DELPHI VFT in a LEP e^+e^- annihilation at $\sqrt{s}$ = 204 GeV (right).

Pixel detectors are the natural successors of the microstrip detector design widely used in high energy physics experiments at fixed target and colliders. By further segmenting the strip implant, truly three-dimensional reconstruction of the point of impact of the ionising particle can be obtained. The read-out is performed by a bump-bonded VLSI chip in hybrid detectors or by integrating the circuitry on the same wafer in the monolithic design.

Hybrid silicon pixel detectors have been developed and successfully applied to track reconstruction in high energy physics experiments in the last decade. In particular, DELPHI at LEP was the first collaboration adopting hybrid pixel sensors for a Vertex Tracker at a collider experiment [19]. The Very Forward Tracker included four crowns of 330 $\times$ 330 μm^2 pixel sensors bump-bonded to read-out VLSI modules for a total of 1.2M channels. The fraction of noisy masked pixels was $\simeq$ 0.3% and the detector efficiency of the order of 95%. Hybrid pixel sensors have been further developed for ALICE [20], ATLAS [21] and CMS [22] to meet the experimental conditions of the LHC collider. These

R&D activities have demonstrated the feasibility of fast time stamping (25 ns) and sparse data scan read-out, and the operability of hybrid pixel detectors exposed to neutron fluxes well beyond those expected at the linear collider.

The linear collider application now defines new areas of specific R&D aimed to improve the achievable single point resolution to better than 10 μm and to reduce the sensor+VLSI thickness. The detector resolution requirement can be accomplished by sampling the diffusion of the charge carriers generated along the particle path and assuming an analog read-out to interpolate the signals of neighbouring cells. Given that the charge diffusion is $\sim$ 8 μm in 300 μm thick silicon, its efficient sampling and signal interpolation requires a pitch of not more than 25 μm. This has been successfully proven to work in one-dimensional microstrip sensors [23]. In pixel devices the ultimate read-

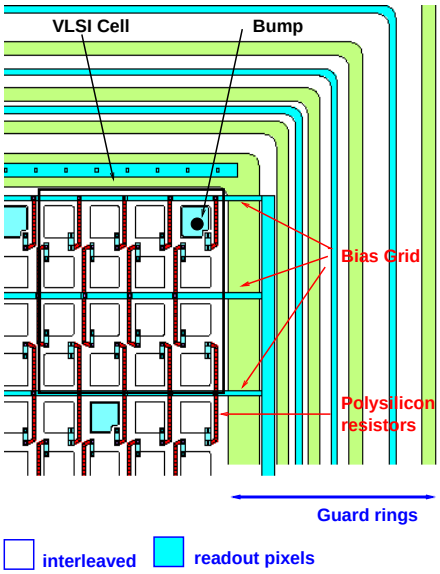

Figure 4: Layout of the upper corner of pixel detector test structure, with 50 μm implant and 200 μm read-out pitch.

out pitch is constrained by the front-end electronics, to be integrated in a cell matching the sensor pattern. At present, the most advanced read-out electronics have a minimum cell dimension of 50×300 μm^2 not suitable for a finely segmented charge sampling. The trend of the VLSI development and recent studies [24] on intrinsic radiation hardness of deep sub-micron CMOS technology certainly allows to envisage of a sizeable reduction in the cell dimensions on a linear collider time scale but sensor designs without such basic limitations are definitely worth being explored. A possible solution is to exploit the capacitive coupling of neighbouring pixels and to have a read-out pitch n times larger than the implant pitch [25]. The proposed sensor layout is shown in Figure 4 for n=4. In this configuration, the charge carriers created underneath an interleaved pixel will induce a signal on the capacitively coupled read-out nodes. In a simplified model, where the sensor is reduced to a capacitive network, the ratio of the signal amplitudes on the read-out nodes at the left- and right-hand side of the interleaved pixel in both dimensions will be correlated to the particle position and the resolution is expected to be better than (implant pitch)/$\sqrt{12}$ for an implant pitch of 25 μm or smaller. The ratio between the inter-pixel capacitance and the pixel capacitance to backplane will play a crucial role, as it defines the signal amplitude reduction at the output nodes and therefore the maximum

number of interleaved pixels. Calculations with such capacitive network models [26] show that resolutions similar to those achieved by reading out all pixels are obtainable if the signal amplitude loss to the backplane is small. Recent tests on a microstrip sensor, with 200 μm read-out pitch, have achieved a 10 μm resolution with three interleaved strip layout [27]. Similar results are expected in a pixel sensor, taking into account both the lower noise because of the intrinsically smaller load capacitance and the charge sharing in two dimensions. Reducing the read-out density, without compromising the achievable space resolution, is also beneficial to limit the power dissipation and the overall costs. In order to verify the feasibility of this scheme a dedicated R&D program has started [28]. A prototype set of sensors with interleaved pixels and different choices of implant and read-out pitch have been already designed, produced and tested[29, 16]. These studies will determine the achievable single point resolution for hybrid pixel sensors.

Monolithic pixel sensors, integrating the read-out circuit on the same silicon wafer acting as particle detector, have been proposed for visible imaging [30] since the beginning of the decade. These devices have several potential advantages including their low cost,

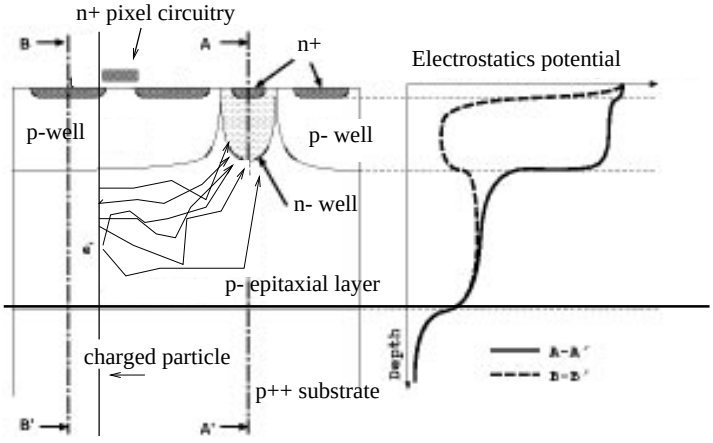

Figure 5: The proposed monolithic pixel structure. The circuitry is integrated in the p-well while the photosite is a n-well diode on the p-epitaxial layer. Because of the difference in doping level, the p-well and the p++ substrate act as reflective barriers. The generated electrons are collected in the n-well.

inherent radiation hardness, possibility to integrate several functionalities on the sensor substrate including random access and very low power consumption since the circuitry in each pixel is only active during read-out time. A limiting factor encountered in visible light applications is the low fill factor, i.e. the fraction of the pixel area that is sensitive to the light. In order to solve this problem for detection of ionising particles, it has recently been proposed to integrate a sensor in a twin-well technology with a n-well/p-substrate diode (see Figure 5) [31]. This technique has already proven its effectiveness in visible light applications [32] reducing the blind area to that of the metal lines, opaque for visible light but not for charged particles. Monolithic CMOS sensors could achieve a high spatial resolution, the achievable pixel pitch being of the order of 10 μm and hence the spatial resolution better than 3 μm already with a binary read-out. At the same time, very low multiple scattering is introduced as the substrate can in principle be thinned down to a few microns. In order to prove the effectiveness of the CMOS sensor technique for the linear collider application, a R&D program has been initiated [33]. Existing commercial

devices are currently under test and the prototype of a full-custom design sensor is being produced in 0.6 μm CMOS technology.

3.2 CCD detectors

Charge coupled devices (CCD) have been successfully used in high resolution tracking detectors both at fixed target and collider experiments since the mid 80's [34]. The first application of CCDs at a collider experiment has been with the VXD1 in the SLD experiment at the SLC collider, later followed by the VXD2 and VXD3 upgrades (see Figure 6). The VXD3 detector consisted of three cylindrical layers, for a total of 307M 20×20 μm^2 pixels providing a space point resolution of 3.8 μm [35]. The read-out time of 180 ms caused the occasional recording of overlapping events. However, due to the low SLC duty cycle and luminosity and the low track density, this did not cause any problems to the track pattern recognition.

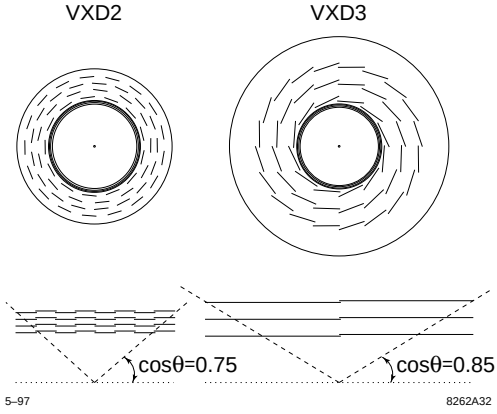

Figure 6: Schematic layouts of the SLD VXD detectors and a magnified view of a candidate $e^+e^- \to Z^0 \to b\bar{b}g$ decay with clearly defined secondary vertices.

For the linear collider application, CCD of larger area (up to 3000 mm^2) and lower thickness (in principle only limited by the epitaxial layer thickness of $\simeq$ 20 μm) are envisaged [36]. Developments in low noise electronics can further improve the single point resolution to $\simeq$ 3 μm. While CCD sensors have ideal characteristics in terms of the spatial resolution and detector thickness, they presently lack the required read-out speed necessary to cope with the TESLA bunch timing and are possibly sensitive to neutron damage at fluxes of the order of that expected at the linear collider. An intense R&D program is presently underway to overcome these limitations [37, 36]. At the read-out speed of 5 MHz, adopted at SLD, the CCD detectors would integrate a full TESLA train of 2850 (4500) bunches at $\sqrt{s}$ = 500 (800) GeV corresponding to 560 (900) hits mm^{-2} and an occupancy of 22 (36)% on the innermost layer. These rates give an unacceptably high number of hit association ambiguities and fake tracks. Even increasing the read-out speed to 50 MHz would not yet provide with a tolerable detector occupancy. In order to solve this problem a new read-out scheme, named "column parallel read-out", has been proposed. In this scheme the serial read-out circuit is replaced by a read-out IC, with circuits every columns, bump-bonded at the end of the CCD ladder (see Figure 7).

The column parallel read-out is aimed at reducing the number of integrated bunches to 60-100, thus achieving an acceptable density of background hits at the innermost layer.

There are further issues deriving from the increased power dissipation and the feasibility to drive CCDs at the proposed frequency that need to be investigated. Also the effect of the high rate of $\gamma\gamma$ overlap to physics events, consequent to the still long integration time of CCD detectors, has still to be studied in details. The CCD sensitivity to radiation damage also requires a careful evaluation. As mentioned above, neutron induced displacements in the bulk silicon create trap regions that reduce the charge transfer efficiency. Due to the several hundreds or thousands of transfers the ionisation charge undergoes before the read-out node, the charge transfer inefficiency (CTI) must be kept below $\simeq 10^{-4}$ not to significantly deteriorate the sensor efficiency. Recent tests of CCD detectors have shown that detector inefficiencies in excess of $\simeq 10\%$ are observed after fluxes of several times 10^9 n (1 MeV) cm^{-2}, unless the detector is cooled to $T < 185°K$ [38]. In fact, at low enough temperature the lifetime of trapped electrons becomes very long and the traps remain filled during the transfer of subsequent electron packets. In addition, the column parallel read-out scheme, decreasing the number of charge transfers before the read-out node, eases the requirements for the maximum tolerable CTI. The radiation resistance of CCD sensors represents a crucial issue in the choice of the detector technology to be reviewed as more experimental data on neutron damage and updates of the final focus region layout and improved neutron flux calculations will become available.

3.3 Conceptual designs

The basic geometrical structure of the Vertex Tracker consists of concentric cylinders of detectors complemented by crowns or disks in the forward regions. In the TESLA design, the first detector layer, closest to the interaction region, is located at a radius of 1.2 cm outside a 0.5 mm thick Be beam-pipe. The beam-pipe is shaped to accommodate the envelope of deflected pairs growing in radius moving away from the interaction region along the beam-line. The distance of the first detector layer from the beam collision point is reduced by more than a factor of 2 compared to that at the SLC and by a factor of 5 compared to LEP to the benefit of the achievable track extrapolation accuracy. Since hybrid pixel detectors and CCDs have different performances in terms of the space resolution and the requirements for mechanical support and cooling, the proposed tracker designs differ accordingly in several details.

The layout of the TESLA Vertex Detector [11] based on hybrid pixel sensors is shown

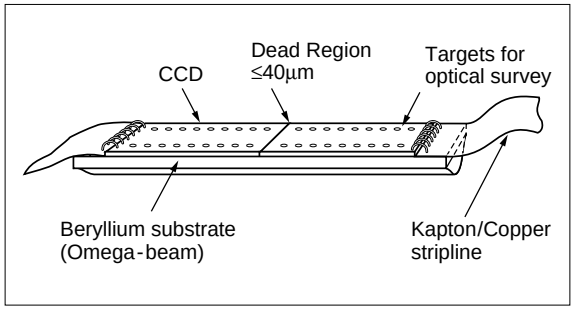

Figure 7: The proposed layout of a CCD ladder (left) with read-out parallel column read-out electronics bump-bonded at one end of the sensitive area (right).

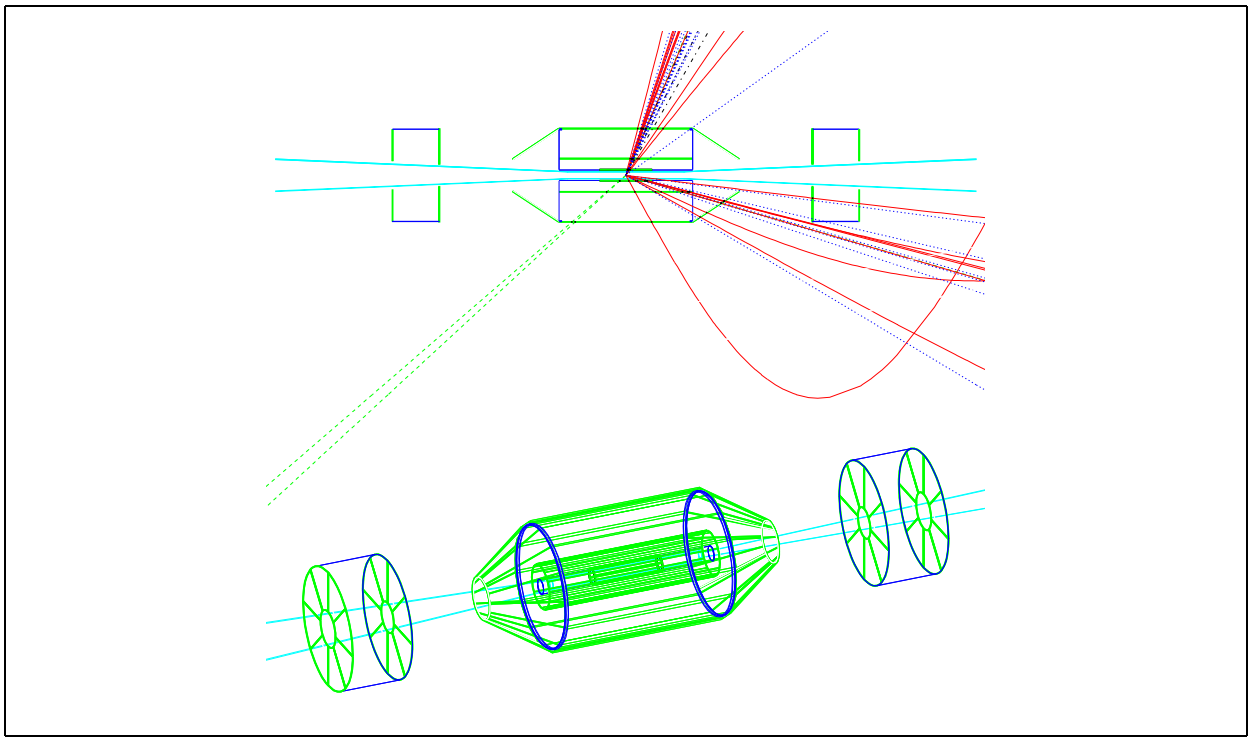

Figure 8: The proposed layout of the Vertex Tracker with a simulated $e^+e^- \rightarrow h^0Z^0 \rightarrow b\bar{b}\mu^+\mu^-$ event overlayed. The three layered barrel section is complemented by a crown and two disks of detectors to ensure accurate tracking in the forward region.

in Figure 8 and consists of a three-layer cylindrical detector surrounding the beam-pipe complemented by forward crowns and disks extending the polar acceptance to small angles following a solution successfully adopted in the DELPHI Silicon Tracker. The three barrel layers have a polar acceptance down to $|\cos\theta| = 0.82$. At lower angles, additional space points are obtained by extending the barrel section by a forward crown and two disks of detectors providing three hits down to $|\cos\theta| = 0.995$. The transition from the barrel cylindrical to the forward conical and planar geometries optimises the angle of incidence of the particles onto the detector modules in terms of the achievable single point resolution and the multiple scattering contribution. Overlaps of neighbouring detector modules provide an useful mean of veryfing the relative detector alignment using particle tracks from dedicated calibration runs taken at Z^0 centre-of-mass energy. The requirement on the multiple scattering contribution to the track extrapolation resolution, lower than 30 μm/p_t, and the need to minimise the amount of material in front of the calorimeters and to ensure the optimal track matching with the main tracking system, set a constraint on the material budget of the Vertex Tracker to less than 3 % of a radiation length (X_0). These requirements can be fulfilled by adopting 200 μm thick detectors and back-thinning of the read-out chip to 50 μm, corresponding to 0.3 % X_0 of a radiation length, and a light support structure. The present concept for the mechanical structure envisages the use of diamond-coated carbon fiber detector support layers acting also as heat pipes to extract the heat dissipated by the read-out electronics uniformly distributed over the whole active surface of the detector. Assuming a power dissipation of 60 μW/channel, the total heat flux is 450 W, corresponding to 1500 W/m^2, for a read-out pitch of 200 μm. Preliminary

results from a finite element analysis show that pipes circulating liquid coolant must be placed every 5 cm along the longitudinal coordinate except for the innermost layer where they can be placed only at the detector ends to minimise the amount of material. Signals can be routed along the beam pipe and the end-cap disks to the repeater electronics installed between the Vertex Tracker and the forward mask protecting the Vertex Tracker from direct and backscattered radiation from the accelerator. The estimated material budget corresponds to 1.6% X_0 for the full tracker.

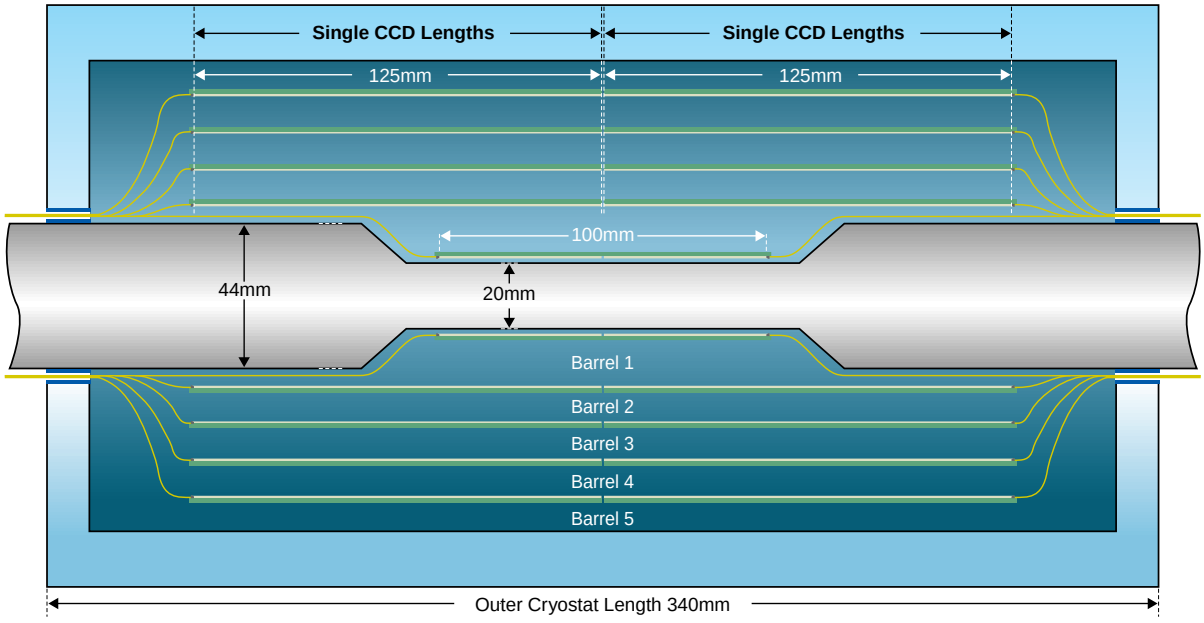

Figure 9: The conceptual design of the CCD Vertex Tracker

The proposed CCD Vertex Tracker consists of five layers of CCD sensors (see Figure 9) providing at least three hits down to $|\cos\theta| = 0.96$ and at least one down to $|\cos\theta| = 0.98$. In the forward region, the track reconstruction relies on the match of the CCD hits with those recorded in disks of pixel detectors similarly to the previous design. The use of five layers of CCD sensors ensures self-consistent tracking capabilities with redundancy. This is possible due to the small multiple scattering contribution expected for thinned sensitive layers on a thin flat Be support structure corresponding to 0.11% X_0/layer. This approach has its point of strength in the higher accuracy that can be achieved in the internal Vertex Tracker alignment, due to the redundant track trajectory measurements, compared to the relative alignment to the main tracking chamber. In addition, the external foam-insulated cryostat can be kept thin enough not to significantly interfere in the linking with the tracks extrapolated from the central tracker towards the vertex. The CCD thinning procedure has been studied in details and finite element analysis has shown that the deformations of the detectors mounted on a properly shaped Be support are within a tolerable range. The total material budget for the CCD Vertex Tracker has been estimated to be 0.70% X_0 plus the cryostat that, however, does not degrade to the track extrapolation accuracy achieved with the Vertex based track fit if the rate of ambiguities is low enough. The light structure and the high accuracy of CCD Vertex detector makes it the most ambitious and performant tracker presently under study.

4 Vertex Tracker performances

The geometry optimisation and the study of the physics performances of the Tracker design has been performed with a GEANT based simulation of the detector, accounting for benchmark physics processes with enhanced forward production cross-section, such as $e^+e^- \rightarrow H^0\nu\bar{\nu}$, pair and $\gamma\gamma$ backgrounds, local pattern recognition and detector inefficiencies. The impact parameter resolution has been obtained by a Kalman filter based track fit to the associated hits in the Vertex Tracker and in the TPC. The impact parameter resolutions, obtained for tracks with $|\cos\theta| < 0.92$, with the Hybrid Pixel and CCD Vertex Tracker options are shown in Figure 10.

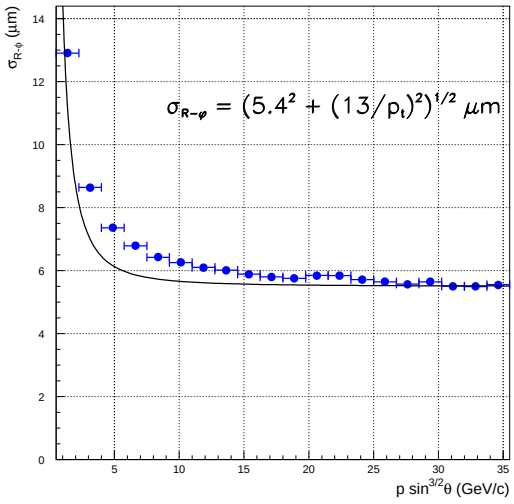

Figure 10: The estimated impact parameter resolution for the Hybrid Pixel (left) and the CCD Vertex Tracker (right), obtained assuming a single point resolution of 7.0 μm and 3.5 μm respectively.

Jet flavour tagging is based on the combination of discriminating variables sensitive to the decay kinematics, the secondary vertex invariant mass and its topology. The combination can be performed defining a combined likelihood, by means of Fischer discriminant or by neural networks exploiting non-linear correlations between the variables. The typical performance for the most demanding flavour tagging task, i.e. the identification of charm, is given in Figure 1. The jet flavour tagging response can be used either as a cut variable for event classification, as an input to a global probability defining the likelihood of the event to be either signal or background or, finally, as fit variable to measure the fraction of decays of a particle, whose properties are under study, in a given flavour configuration.

The impact of the Vertex Tracker on the physics studies at the linear collider can be exemplified by the results on the determination of the Higgs decay branching ratios. For its own importance in the study of the properties of the Higgs boson and also for its requirements to jet flavour identification, this process has been adopted as one of the main benchmark reaction for the optimisation of the Vertex Tracker design. The scenarios with a 120 GeV/c^2 or a 140 GeV/c^2 neutral Higgs boson have been studied for an integrated luminosity of 500 fb^{-1} at $\sqrt{s} = 350$ GeV and 500 GeV. A jet flavour tagging algorithm has been applied to the di-jets originating from the Higgs decay in the Higgsstrahlung process

$e^+e^- \rightarrow Z^0H^0$. The fractions of $b\bar{b}$, $c\bar{c}$ and gg decays have been extracted by a binned maximum likelihood fit to the jet flavour tagging probability distribution. The results are summarised in Figure 11. The estimated accuracy allows to distinguish the nature of a neutral Higgs boson, telling a Minimal Supersymmetric Standard Model (MSSM) Higgs from the Standard Model one, for values of the heavy A^0 boson mass up to $\simeq 600$ GeV/c^2 independent on the value of $\tan\beta$ [6, 39]. This region is particularly important because it corresponds to the portion of the MSSM parameter space where the LHC experiments may only be able to observe one Higgs boson without establishing its Supersymmetric or Standard Model nature.

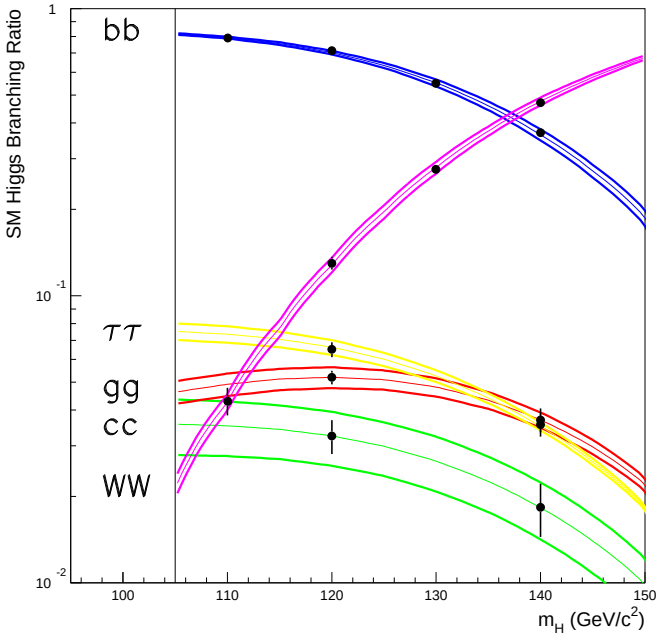

Figure 11: The predicted SM Higgs decay branching ratios shown as the 68% confidence level bands with overlayed the measured points using the results of this study (from Ref. [6]).

5 Conclusions

The linear collider physics programme defines challenging requirements for the Vertex Tracker. The solutions presently considered for the TESLA project, rely on the experience with the LEP/SLC detectors, the results of the LHC R&D and those of dedicated activities. The estimates for the backgrounds at the interaction region and their degree of uncertainty motivate different sensor technology to be studied. Pixel sensors guarantee a stable operation in the interaction region environment however they presently lack the necessary accuracy and thinness. In order to overcome these limitations R&D on hybrid sensors of new design, with interleaved pixels, and monolithic CMOS sensors is being carried out. CCD devices offer the most attractive performances in this respect while they require further R&D to demonstrate their full compatibility with the accelerator timing

and backgrounds. The availability of alternative detector technologies allows to emphasise different aspects of experimentation at the linear collider. The tracker design and the detector technology will evolve with the results of R&D, physics studies and updates of accelerator parameters towards the definition of the most performant Vertex Tracker ever designed. Preliminary evaluations of the performance and of the physics reach define a rich variety of signals of new physics and of precision measurements relying on the Vertex Tracker resolution.

6 Acknowledgements

We thank our collegues of the Helsinki, Milano, Krakow and Strasbourg groups for their contributions to the different stages of the studies reviewed in this paper. We want to express our gratitude to Chris Damerell for many stimulating discussions and his valuable suggestions. One of the authors (M.B.) is also thankful to Goran Jarlskog and Leif Jonsson for their kind invitation to the Lund Workshop.

References

[1] Reviews of the linear collider physics program are given in E. Accomando *et al.*, *Phys. Rep.* **299** (1) (1998), 1 and in P. Zerwas, contribution to these Proceedings.

[2] For a review of the general detector concept and its expected performances see R. Heuer, contribution to these Proceedings.

[3] E. Gross, to appear in Proc. of the *Int. Europhysics Conference on High Energy Physics*, Tampere (Finland), July 1999.

[4] H.E. Haber, in Proc. of the 4^{th} *Int. Conf. on Physics beyond the Standard Model*, Lake Tahoe, (USA); World Scientific, Singapore, 1995;
J. Kamoshita, Y. Okada and M. Tanaka, in Proc. of the *Workshop on Physics and Experiments with Linear Colliders*, eds. A. Miyamoto *et al.*, Morioka (Japan); World Scientific, Singapore, 1996.

[5] M.D. Hildreth, T.L. Barklow and D.L. Burke, *Phys. Rev. Lett.* **49** (1994) 3441.

[6] M. Battaglia, to appear in Proc. of the *Int. Workshop on Linear Colliders LCWS99*, Sitges (Spain), May 1999 and hep-ph/9910217.

[7] for recent reviews of these activities see the contributions by J. Brau, M. Caccia, T. Greenshaw, Y. Sugimoto and H. Yamamoto to the Proc. of the *Int. Workshop on Linear Colliders LCWS99*, Sitges (Spain), May 1999.

[8] R. Brinkmann, G. Materlik, J. Rossbach, A. Wagner (ed.), *Conceptual Design of 500 GeV e^-e^+ Linear Collider with Integrated X-ray Laser Facility*, DESY 97-048.

[9] D. Schulte, contribution to these Proceedings.

[10] M.S. Zolotarev, E.A. Kuraev and V.G. Serbo, Inst. Yadernoi Fiziki Preprint, 81-63 (1981), translated as SLAC TRANS-227 (1987).

[11] M. Battaglia *et al.*, in Proc. of the 2^{nd} *Workshop on Backgrounds at the Machine Detector Interface*, eds. T.E. Browder and S.K. Sahu, Honolulu HI (USA), 1997; World Scientific, Singapore 1998 and in DESY 97-123E.

[12] N. Tesch, to appear in Proc. of the *Int. Workshop on Linear Colliders LCWS99*, Sitges (Spain), May 1999.

[13] M. Battaglia and S. Ye, HIP-1999-73/EXP.

[14] H. Yamamoto, to appear in Proc. of the *Int. Workshop on Linear Colliders LCWS99*, Sitges (Spain), May 1999.

[15] M. Battaglia *et al.*, to appear in Proc. of the *Vertex99 Workshop*, Texel (The Netherlands), June 1999 and hep-ex/9911013.

[16] M. Caccia *et al.*, to appear in Proc. of the *Int. Workshop on Linear Colliders LCWS99*, Sitges (Spain), May 1999 and hep-ex/9910019.

[17] C.J.S. Damerell and D.J. Jackson, in Proc. of the *APS Workshop on New Directions for High Energy Physics*, Snowmass (USA), July 1996.

[18] D. Di Bari *et al.*, *Nucl. Instr. and Meth.* A 395 (1997) 391.

[19] P. Chochula *et al.*, *Nucl. Instr. and Meth.* A 412 (1998) 304.

[20] F. Antinori, in Proc. of the *Int. Pixel Detector Workshop PIXEL98*, FERMILAB-CONF 98-196, 41.

[21] ATLAS collaboration, *The Pixel Detector Technical Design Report*, CERN-LHCC 98-13.

[22] D. Bortoletto, in Proc. of the *Int. Pixel Detector Workshop PIXEL98*, FERMILAB-CONF 98-196, 22.

[23] U. Kötz *et al.*, *Nucl. Instr. and Meth.*, A 235 (1985), 481.

[24] W. Snoeys, CERN–LHCC 97-60, 139.

[25] V. Bonvicini and M. Pindo, *Nucl. Instr. and Meth.* A 372 (1996) 93.

[26] M. Pindo, *Nucl. Instr. and Meth.* A 378 (1996) 443.

[27] M. Krammer and H. Pernegger, *Nucl. Instr. and Meth.* A 397 (1997) 232.

[28] This R&D program is carried out by the University of Helsinki, the University of Mining and Metallurgy and the Institute of Nuclear Physics in Krakow, the University of Milano and the Institute of Electron Technology in Warsaw.

[29] W. Kucewicz *et al.*, *Acta Phys. Pol.* B 30 (1999) 2075.

[30] E.R. Fossum, *IEEE Trans. Electron Devices*, 41 (1994), 452.

[31] R. Turchetta, presentation at the 2nd SOCLE Meeting, Paris (France), January 28, 1999

[32] B. Dierickx, G. Meynants, D. Scheffer, in Proc. of the *IEEE CCD & AIS Workshop*, Brugge, Belgium, June 1997.

[33] This R&D program is carried out by the Institut de Recherches Subatomique and the Laboratoire d'Electronique et de la Physique des Systemes Instrumentaux in Strasbourg.

[34] C.J.S. Damerell *et al.*, *IEEE Trans. Nucl. Sci.* **33** (1986), 51.

[35] K. Abe *et al.*, *Nucl. Instr. and Meth.* A 400 (1997), 287.

[36] T. Greenshaw *et al.*, to appear in Proc. of the *Int. Workshop on Linear Colliders LCWS99*, Sitges (Spain), May 1999;
P. Burrows, to appear in Proc. of the *Vertex99 Workshop*, Texel (The Netherlands), June 1999 and hep-ex/9908004.

[37] This R&D program is carried out by the LCFI (UK) Collaboration formed by the Brunel, Glasgow, Lancaster, Liverpool and Oxford Universities and the Rutherford Appleton Laboratory.

[38] Contributions by J. Brau and Y. Sugimoto to appear in Proc. of the *Int. Workshop on Linear Colliders LCWS99*, Sitges (Spain), May 1999.

[39] G. Borisov and F. Richard, LAL 99-26 and hep-ph/9905413.